

Imidazole C-2 Hydrogen/Deuterium Exchange Reaction at Histidine for Probing Protein Structure and Function with Matrix-Assisted Laser Desorption Ionization Mass Spectrometry

Naoka Hayashi,[†] Hiroki Kuyama,[‡] Chihiro Nakajima,[‡] Kazuki Kawahara,[§] Masaru Miyagi,^{||} Osamu Nishimura,[‡] Hisayuki Matsuo,[⊥] and Takashi Nakazawa^{*,†}

[†]Department of Chemistry, Nara Women's University, Nara 630-8506, Japan

[‡]Institute for Protein Research, Osaka University, Suita, Osaka 565-0871, Japan

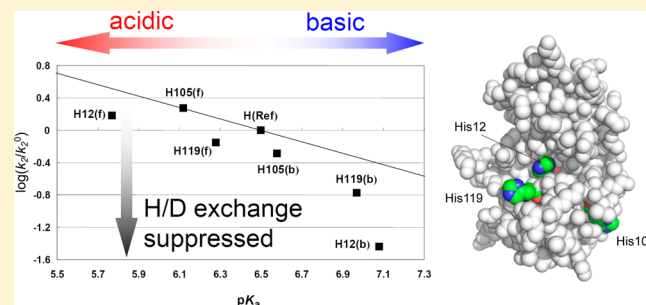
[§]Graduate School of Pharmaceutical Sciences, Osaka University, Suita, Osaka 565-0871, Japan

^{||}Case Center for Proteomics and Bioinformatics, Department of Pharmacology, and Department of Ophthalmology and Visual Sciences, Case Western Reserve University, 10900 Euclid Avenue, Cleveland, Ohio 44106-4988, United States

[⊥]National Cerebral and Cardiovascular Center Research Institute, Suita, Osaka 565-8565, Japan

Supporting Information

ABSTRACT: We present a mass spectrometric method for analyzing protein structure and function, based on the imidazole C-2 or histidine C^{ε1} hydrogen/deuterium (H/D) exchange reaction, which is intrinsically second-order with respect to the concentrations of the imidazolium cation and OD[−] in D₂O. The second-order rate constant (k_2) of this reaction was calculated from the pH dependency of the pseudo-first-order rate constant (k_p) obtained from the change in average mass [ΔM_r ($0 \leq \Delta M_r < 1$)] of a peptide fragment containing a defined histidine residue at incubation time (t) such that $k_p = -[\ln(1 - \Delta M_r)]/t$. We preferred using k_2 rather than k_p because k_2^{\max} (maximal value of k_2) was empirically related to pK_a as illustrated with a Brønsted plot [$\log k_2^{\max} = -0.7pK_a + \alpha$ (α is an arbitrary constant)], so that we could analyze the effect of structure on the H/D exchange rate in terms of $\log(k_2^{\max}/k_2)$ representing the deviation of k_2 from k_2^{\max} . In the catalytic site of bovine ribonuclease A, His12 showed a change in $\log(k_2^{\max}/k_2)$ much larger than that of His119 upon binding with cytidine 3'-monophosphate, as anticipated from the X-ray structures and the possible change in solvent accessibility. However, we need to consider the hydrogen bonds of the imidazole group with nondissociable groups to interpret an extremely slow H/D exchange rate of His48 in a partially solvent-exposed situation.



Hydrogen/deuterium (H/D) exchange is an invaluable tool for probing the dynamic structure and interaction of macromolecules.^{1,2} Amide hydrogen atoms in the polypeptide backbone have been exploited extensively as probes because of their ubiquitous distribution over the whole protein molecule. Techniques for studying such H/D exchange phenomena in proteins include nuclear magnetic resonance (NMR) spectroscopy and electrospray ionization mass spectrometry (ESI-MS), taking advantage of their abilities to assign resonances or peaks to individual exchanging sites with high resolution and to reproduce “near-native” solution conditions in sample preparations and measurements. For large proteins to which NMR cannot be applied, ESI-MS is still useful for conducting the H/D exchange experiments with its high sensitivity and ease of assignment. However, the amide N H/D exchange proceeds so fast that the technical demands for suppressing the back-exchange reaction and scrambling among many amide N H(D) sites are quite heavy.

Compared with amide NH groups, the C^{ε1} hydrogen of the histidine residue undergoes H/D exchange at a much slower

rate with a half-life on the order of days,³ because of the covalent nature of the C–H bond. One of the notable features of this C^{ε1} H/D exchange reaction is that only the protonated imidazolium form in equilibrium with the neutral imidazole can react with the hydroxyl (OD[−]) ion to give a ylide or a carbene intermediate at the rate-determining step (Scheme 1).^{4–6}

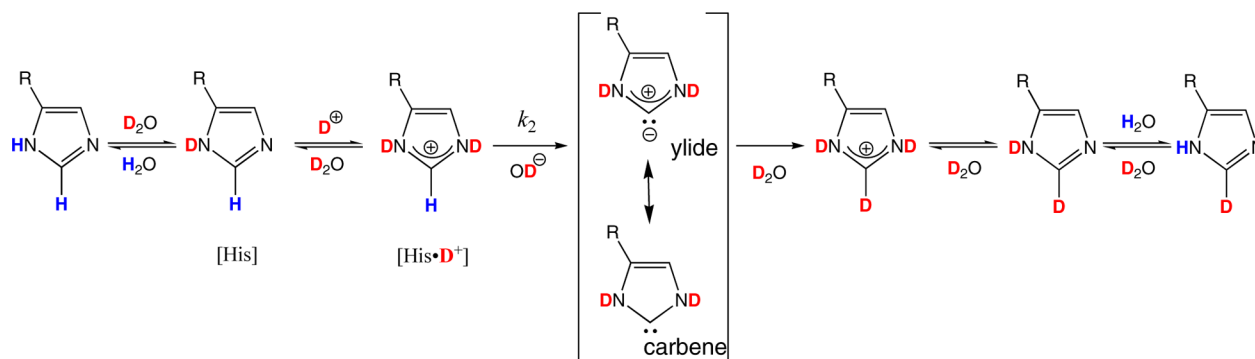
The pK_a value of the imidazole group at the side chain of a histidine residue can therefore be measured from the pH (pD) dependency of the pseudo-first-order rate constant (k_p) for the H/D exchange reaction. In line with this principle, a method for determining the pK_a value of each histidine residue in proteins was developed in archetypal studies of the hydrogen/tritium (H/T) exchange reaction.^{7,8} Because of the frequent involvement of the imidazole group in enzyme catalysis as both an acid and a base, the H/T or H/D exchange method in

Received: September 10, 2013

Revised: March 6, 2014

Published: March 7, 2014



Scheme 1. Mechanism of the H/D Exchange Reaction at the C^{ε1} Position of a Histidine Residue in D₂O^a


^aThe reaction of His-D⁺ (protonated form of the imidazole group) with the OD⁻ ion is rate-determining such that v (reaction rate) = k_2 [His-D⁺][OD⁻]. The N^{δ1} and N^{ε2} (ring N-1 and N-3, respectively) deuterium atoms are back-exchanged with hydrogen atoms much faster than the C^{ε1} deuterium atom in light water (H₂O). The concentration of the neutral N^{ε2}-D tautomer (not illustrated) of histidine is included in [His].

conjunction with then emerging ¹H NMR spectroscopy has proven to be the most reliable technique for determining pK_a values of individual histidine residues in proteins.^{3,9} Although we have elaborated the much simpler H/D exchange technique aided by liquid chromatography (LC)–ESI-MS to reduce the difficulties inherent in performing the H/T exchange experiment with radioactive tritium,¹⁰ there remains the difficulty of interpreting the maximal pseudo-first-order rate constant (k_{ϕ}^{\max}) in terms of solvent accessibility.⁷ This is due to the explicit dependency of k_{ϕ}^{\max} on pK_a, unlike that of the corresponding kinetic parameter of the amide N H/D exchange reaction. One of the most promising approaches to addressing this issue is to use a linear free energy relationship between pK_a and the second-order rate constant (k_2),¹¹ which derives from the experimental value of k_{ϕ}^{\max} and pK_a. Indeed, the preceding H/T exchange experiments demonstrated the utility of a Brønsted plot to assess the effect of protein structure on the k_2 and pK_a values of histidine residues in bovine heart cytochrome *c* and RNase St.^{12,13} We therefore adapted the concept of the linear free energy relationship into the mass spectrometric histidine C^{ε1} H/D exchange method for utilizing the imidazole groups as probes to study the noncovalent interactions and structural dynamics of proteins, as exemplified by renowned amide N H/D exchange approaches. This would alleviate the difficulty that often arises when we try to compare the solvent accessibilities of two histidine residues via their half-lives ($t_{1/2}$),^{14,15} which are related to k_{ϕ}^{\max} through the formula $t_{1/2} = (\ln 2)/k_{\phi}^{\max}$.

In addition to the adaptation of the linear free energy relationship expressed by a Brønsted equation to interpret kinetic data of the H/D exchange reaction, we extend the method to be applied to virtually every protein sample by employing matrix-assisted laser desorption/ionization (MALDI) MS as well as LC–ESI-MS. One of the advantages of MALDI MS is that it is faster because the identification and characterization of all the peptide peaks can be performed simultaneously. Omitting the repetitive procedure of LC separation can greatly enhance the throughput of the analysis. Its possible drawback is that not all the molecular ions are detected with a sufficiently high signal-to-noise (S/N) ratio in a single MALDI spectrum. To address this issue, we elaborated a new data-processing scheme based on the calculation of a weighted average (M_r) of isotopic peaks. Although the increment of M_r is within 1 Da during the H/D exchange reaction at each histidine C^{ε1} site, it is possible to monitor a

mass shift of <0.1 Da or very close to 1 Da, irrespective of the value of M_r .

We illustrate a new protocol adapted to MALDI MS in the measurement of histidine C^{ε1} H/D exchange reaction rates in bovine pancreatic ribonuclease A (RNase A), the enzyme examined in our previous study using LC–ESI-MS.¹⁰ On the basis of a linear free energy relationship between log k_2 and pK_a,¹³ we analyzed the inhibitory effect of cytidine 3′-monophosphate (3′-CMP) on RNase A with respect to the acid–base character and solvent accessibility of histidine residues, especially His12 and His119 interacting directly with 3′-CMP at the active site. We suggest that solvent accessibility is not a sole factor responsible for determining the H/D exchange rate, based on the X-ray crystallographic structure of RNase A, in which the C^{ε1} H of His48 undergoes H/D exchange extremely slowly while it is not completely shielded from solvent but involved in a network of hydrogen bonds.

EXPERIMENTAL PROCEDURES

Materials. Deuterium oxide (D₂O, 99.9%) was purchased from Cambridge Isotope Laboratories (Andover, MA), and deuterium chloride (DCl) and sodium deuteroxide (NaOD) were from Sigma-Aldrich (St. Louis, MO). Bovine pancreatic ribonuclease A (RNase A), cytidine 3′-monophosphate (3′-CMP) monosodium salt, trypsin, chymotrypsin, and subtilisin (Carlsberg) were obtained from Sigma-Aldrich and used without further purification. α -Cyano-4-hydroxycinnamic acid (CHCA; high-purity MS grade) was purchased from Shimadzu GLC (Tokyo, Japan). Methanediphosphonic acid (MDPNA) was obtained from Tokyo Chemical Industry (Tokyo, Japan). All other chemicals and materials were reagent grade or of the highest quality.

Methods. Buffer Solutions in D₂O. Buffers used for H/D exchange were 50 mM sodium acetate (pH 3.5–4.5), 50 mM MES (pH 5.0–7.5), and 50 mM HEPES (pH 8.0–9.0) in D₂O. The pH of the buffers was adjusted with diluted DCl or NaOD and measured with a Horiba (Kyoto, Japan) pH meter F7 equipped with an ultramicro glass electrode (Fuji Chemical Measurement, Tokyo, Japan). The reported pH values are direct pH meter readings of the D₂O buffer solutions calibrated with standard buffer solutions made with H₂O and are uncorrected for the isotope effect at the glass electrode. The ionic strength of the buffers was standardized with pH 4.5 buffer consisting of 50 mM MES and 50 mM NaCl, which had a conductivity value of 4.5 mΩ/cm. The pH of the solution was

measured before and after the H/D exchange reaction and reported as the mean value.

H/D Exchange Reaction of RNase A and Sample Preparation for the Measurement of Mass Spectra. A powder of RNase A (12.5 nmol) was dissolved in an appropriate buffer (100 μ L) to make a 0.125 mM solution in D₂O. The quantity of 3'-CMP in this solution was 37.5 nmol (2.5-fold molar excess with respect to RNase A). The solution in an Eppendorf tube (tightly capped to avoid contamination with H₂O) was incubated at 37 °C for 48 h. After the reaction, the solution was divided into two equal portions (i and ii) to obtain the requisite set of histidine-containing peptides by digesting the enzyme with different proteases. Solution i was acidified to terminate the reaction by the addition of formic acid (10 μ L), followed by removing salts using a Microcon centrifugal filter [10 kDa cutoff (Millipore, Bedford, MA)]. The protein that remained after evaporation of the solvent with a SpeedVac was dissolved in a 5:1 formic acid/methanol mixture (50 μ L), subjected to oxidation with performic acid generated *in situ* in a 95:5 mixture of formic acid and 30% aqueous hydrogen peroxide (50 μ L), and allowed to stand for 2.5 h in an ice bath. The solution was diluted with cold water (500 μ L) and evaporated to dryness with a SpeedVac. The oxidized protein was dissolved in 0.1 M ammonium bicarbonate (20 μ L) and digested successively with trypsin (7 μ g) and chymotrypsin (7 μ g) for 1 h each at 37 °C. Prior to the measurement of mass spectra (next section), the peptides were adsorbed on a ZipTip_{C18} (Waters, Bedford, MA) and then eluted three times with 50% aqueous acetonitrile (10 μ L each) containing 0.1% trifluoroacetic acid (TFA). In solution ii, intact and H/D-exchanged RNase A was digested with subtilisin (2 μ g) for 3 h in an ice bath at pH 8.0 (ammonium bicarbonate) to obtain the S-peptide [RNase A(1–20)] containing His12, according to the standard protocol.¹⁶ The resulting digest was acidified with 10% formic acid (2 μ L) and subjected to MS after desalting using a ZipTip_{C18} (Waters) and eluting three times with 50% aqueous acetonitrile (10 μ L each) containing 0.1% TFA.

Mass Spectrometry (MALDI-TOF MS and MALDI-PSD MS). MALDI-TOF mass spectra were recorded using an AXIMA Performance (Shimadzu/Kratos, Manchester, U.K.) instrument. A nitrogen laser (337 nm, 3 ns pulse width) was used to irradiate the sample for ionization. The accelerating voltage of the instrument was set to 20 kV using a gridless-type electrode. In reflectron mode set to detect positive ions, each spectrum was obtained by accumulating 150–250 laser shots. We chose the saturated solution of CHCA as a matrix in 50% aqueous acetonitrile containing 0.05% TFA. To suppress the appearance of peaks as adducts with alkali metal ions, a 2% aqueous solution of MDPNA was added to the solutions of the matrix and samples.¹⁷ A portion (0.4 μ L) of each sample solution was mixed with the same (0.4 μ L) volumes of matrix and additive solutions on the MALDI target and analyzed after being dried. The *m/z* values of spectra were externally calibrated with CHCA and angiotensin II.

Processing of Mass Spectrometric Data To Calculate the Rate Constant (k_ϕ). When the H/D exchange reaction occurs at the C^ε1 position of a histidine, the average mass (M_r) of the peptide containing one histidine residue should increase by 1 Da because of the difference between isotopic masses m_D (2.014101 Da) and m_H (1.007825 Da) for deuterium and hydrogen atoms, respectively, upon completion of the reaction. This process has proven to follow first-order kinetics, as expressed by the equation

$$\begin{aligned} M_r(t) - M_r(0) &= (m_D - m_H)[1 - \exp(-k_\phi t)] \\ &= 1 - \exp(-k_\phi t) \end{aligned} \quad (1)$$

in which the apparent average mass at time t [$M_r(t)$] is related to that at time zero [$M_r(0)$] through the pseudo-first-order rate constant (k_ϕ), taking $m_D - m_H = 1$ as a good approximation to 1.00628. For the experiment to be performed with a solvent in which the D₂O content (p) is given by $p = [D_2O]/([H_2O] + [D_2O]) \leq 1$, the term $m_D - m_H$ in eq 1 should be replaced with $p(m_D - m_H)$. In addition, if we consider that there are p (>1) sites undergoing the H/D exchange reaction with an average rate constant (k_ϕ)_{av}, eq 1 incorporating the term p should have essentially the same form as that used in a SUPREX method based on the H/D exchange reaction for probing protein–ligand interactions.^{15,18} Although it is difficult to measure the mass-to-charge ratio (*m/z*) for $M_r(0)$ and $M_r(t)$ very accurately and independently, the difference $M_r(t) - M_r(0)$ can be obtained exclusively from the shift in the patterns of isotopic peaks. This is because an average mass M_r is the sum of monoisotopic mass M and the weighted average of isotopic peak intensities as follows:

$$\begin{aligned} M_r(t) &= \frac{\sum_{i=0}^n (M + i)I_{M+i}(t)}{\sum_{i=0}^n I_{M+i}(t)} \\ &= M + \frac{\sum_{i=0}^n iI_{M+i}(t)}{\sum_{i=0}^n I_{M+i}(t)} \left[\bar{I}_{M+i}(t) \equiv \frac{I_{M+i}(t)}{\sum_{i=0}^n I_{M+i}(t)} \right] \\ &= M + \sum_{i=0}^n i\bar{I}_{M+i}(t) \end{aligned} \quad (2)$$

Taking the difference $M_r(t) - M_r(0)$ removes time-independent value M from eqs 1 and 2. We thus obtain the following equation, which involves only relative peak intensity $\bar{I}_{M+i}(t)$ and an integer i as variables.

$$k_\phi t = -\ln \left\{ 1 - \left[\sum_{i=0}^n i\bar{I}_{M+i}(t) - \sum_{i=0}^n i\bar{I}_{M+i}(0) \right] \right\} \quad (3)$$

In the preceding study, we derived a similar equation:¹⁰

$$k_\phi t = \ln \left[1 - \frac{I_{M+1}(0)}{I_M(0)} + \frac{I_{M+1}(0)}{I_M(t)} \right] \quad (4)$$

based on the same kinetics as in eq 3, while taking just two variables, I_M and I_{M+1} , into account. Despite the formal similarity, there is a large difference in the involvement of the nonlinear term I_{M+1}/I_M in eq 4, which would be seriously susceptible to interference unevenly imposed by background noise or spectral artifacts on either the denominator or the numerator, especially in cases in which $I_{M+1} \gg I_M$ and $I_{M+1} \ll I_M$. The details of the derivation of eqs 1–3 are given in the Supporting Information.

The plot of k_ϕ versus pH results in a titration curve, which should be sigmoidal in the form of the Henderson–Hasselbalch equation (eq S-I-8 of the Supporting Information):

$$\log \left(\frac{k_\phi^{\max} - k_\phi}{k_\phi} \right) = pK_a - pH \quad (5)$$

In this titration curve, k_ϕ varies from 0 to k_ϕ^{\max} from the acidic (pH \ll pK_a) to alkaline (pH \gg pK_a) regions, respectively, with

the midpoint at $k_{\phi} = k_{\phi}^{\max}/2$ and $\text{pH} = \text{pK}_a$. Note that each value of k_{ϕ} is obtained as a slope of the line represented by eq 3, which requires the measurement of at least two data points at times zero and, for example, 48 h as we have taken in this study. We repeated the measurement of k_{ϕ} three times at each pH. Although it is also possible to calculate the initial isotopic distribution $\bar{I}_{M+i}(0)$ from the chemical formula,¹⁵ the corresponding experimental value deviated substantially from the theoretical one. We therefore determined the initial value by taking the average of all the experimental data points of $\bar{I}_{M+i}(0)$ for each histidine residue. The slope k_{ϕ} could be obtained more precisely by sampling data at an increased number of time intervals. We applied a nonlinear least-squares fit to a sigmoidal curve of k_{ϕ} versus pH in the form of eq 5 to determine k_{ϕ}^{\max} and pK_a values as described previously.¹⁰ The standard deviation in k_{ϕ} and the variation of pH during the H/D exchange reaction (up to approximately ± 0.15 pH unit) were ignored in the curve fitting.

RESULTS AND DISCUSSION

Sample Preparation. In the preceding paper describing this method using LC–ESI–MS, all the histidine-containing peptides for determining pK_a and k_{ϕ} values could be obtained by successive digestion with trypsin and chymotrypsin, followed by separation by LC. Each peptide thus separated was directly subjected to ESI–MS to determine the H/D exchange rate constant at a given pH.¹⁰ Expecting to detect and analyze the four peaks of histidine-containing peptides simultaneously, we directly submitted the mixture of peptides to MALDI MS. This avoided the need for LC separation to be run as many times as the number of pH values to be plotted on a titration curve. Eventually, three of four peaks, each of which represents a peptide containing one histidine residue (Figure S1 of the Supporting Information), could be submitted to proper processing to obtain individual k_{ϕ} values. However, the peak of peptide QHM*DSSTSAASSNY (M*, methionine sulfone) containing His12 was not detectable at the expected mass value of 1603.6 Da. Instead, the peak of this peptide in the N-terminal pyroglutamyl form was observed infrequently and only marginally; it was not intense enough for measurement of the k_{ϕ} value. Fortunately, His12 is the sole histidine residue in the S-peptide (KETAAKFERQHMDSSSTAA), which derives from native RNase A by a specific proteolytic cleavage between residues 20 and 21 with subtilisin.¹⁶ Because of this highly efficient cleavage, the desired isotopic peaks of the S-peptide (monoisotopic peak at m/z 2166.5) could be detected with a sufficiently high S/N ratio in all the spectra to determine the H/D exchange rate at varied pH values (Figure 1).

In this experiment, special care was taken to suppress the back-exchange of histidine $\text{C}^{\epsilon 1}$ D, while allowing labile deuterons to exchange back to protons during the proteolytic digestion in H_2O before the peptides were subjected to MALDI MS. Although the H/D exchange rate of the histidine $\text{C}^{\epsilon 1}$ proton is overwhelmingly slower than that of the amide NH proton as well as the rates of other labile protons, exposing proteins even to a modestly alkaline condition for a long period of time could cause undesirable back-exchange. The possible error due to the back-exchange (D/H) is $<4\%$ of the rate constant during the enzyme digestion of the protein for 2 h at 37°C and pH 8 in comparison with the incubation for 48 h in H/D exchange. This suggests that the experimental error should be less significant in the limited proteolysis of native RNase A with subtilisin to yield the S-peptide at a temperature

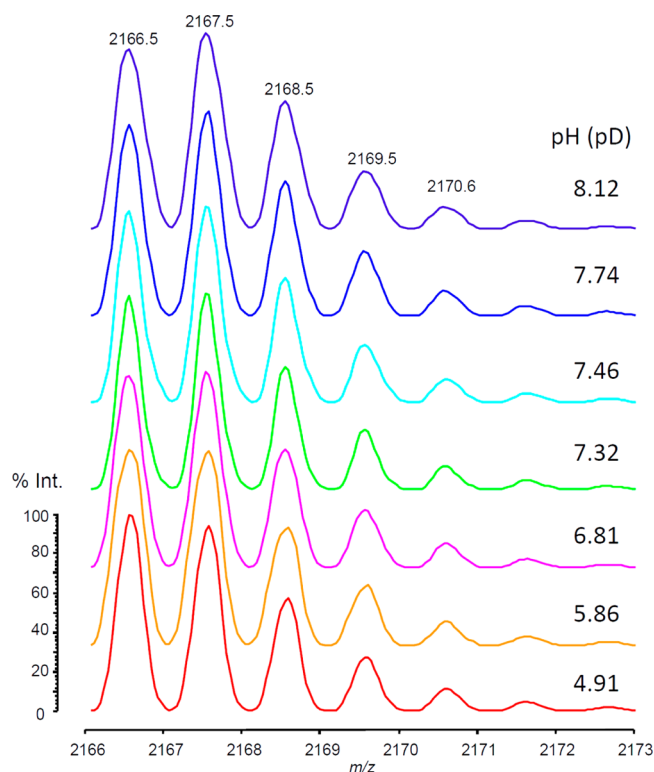


Figure 1. Effect of pH-dependent H/D exchange on the isotopic pattern of MALDI–TOF mass spectra of the RNase A S-peptide. The intensity of the monoisotopic peak at m/z 2166.5 corresponds to $I_M(t)$, and those of peaks up to m/z 2170.6 for $I_{M+4}(t)$ were used for the calculation of k_{ϕ} via eq 3. Individual traces are picked out from the data taken at 48 h and employed for the plot of k_{ϕ} vs pH in Figure 2C of RNase A in the presence of 3'-CMP. Although the general appearances of these spectra are quite similar, the change in the relative intensities of peaks I_M ($i = 0$) and I_{M+1} ($i = 1$) is conspicuous. For the more drastic change in the isotope pattern observed for His105, see Figure S2 of the Supporting Information.

very close to 0°C at pH 8. Pepsin cleaves peptide bonds under acidic conditions where back-exchange of histidine $\text{C}^{\epsilon 1}$ D is least likely to occur, so that it is potentially preferable to alkaline proteases.

Measurement of k_{ϕ} and pK_a of Histidine Residues in RNase A. As illustrated in Figure S1 of the Supporting Information, the peaks of histidine-containing peptides were detected with varied intensities in a MALDI mass spectrum. Despite the relatively poor S/N ratio of the peak at m/z 1263.6 for a peptide containing His105, the values of k_{ϕ} processed by eq 3 converged into a titration curve, in which the midpoint of the sigmoid and the plateau representing the pK_a and k_{ϕ}^{\max} values, respectively, could be discerned (Figure 2). The results of the measurements are summarized in Table 1. For the peptide containing His48, however, there appeared to be no noticeable pH dependency of k_{ϕ} even when the incubation time for H/D exchange was prolonged for up to 7 days and the intensities of the relevant isotopic peaks were comparable with those of the His119-containing peptide. This is partly due to the considerably low solvent accessibility of this residue with a k_{ϕ}^{\max} of $5 \times 10^{-4} \text{ h}^{-1}$ or a half-life of 58 days determined by the previously described H/T exchange method.⁷ Comparing these results, we conclude that the calculation with eq 3 is susceptible to noise peaks to a lesser extent than that with eq 4, probably because it can effectively attenuate noise spikes through

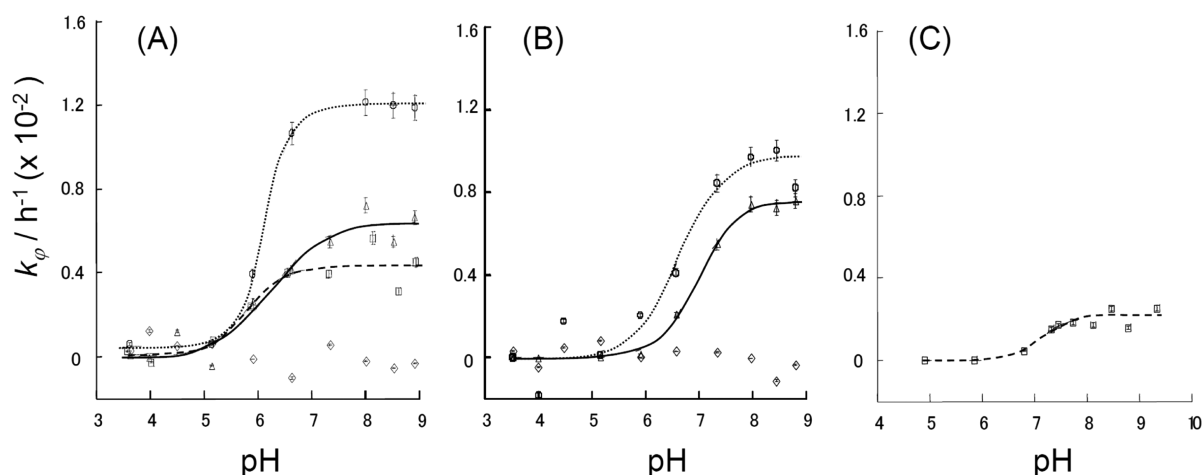


Figure 2. Plot of k_ϕ vs pH in the measurement of pK_a and k_ϕ^{\max} values for histidine residues in RNase A. (A) Titration curves for His119 (\triangle , solid line), His105 (\circ , dotted line), and His12 (\square , broken line) in the absence of 3'-CMP, (B) those for His119 and His105 in the presence of 3'-CMP, and (C) that for His12 in the presence of 3'-CMP. In panel C, the peptide containing His12 was prepared by limited proteolysis of RNase A with subtilisin. His48 (\diamond) gave the data points scattered around the bottom of panels A and B, making it impossible to draw a line or fit them to a defined curve. Error bars represent the standard deviation based on triplicate experiments.

Table 1. Parameters Obtained via Characterization of the H/D Exchange Reaction of Histidine Residues in RNase A^a

parameter ^b	His12		His105		His119	
	free	with 3'-CMP	free	with 3'-CMP	free	with 3'-CMP
pK_a	5.77 ± 0.03	7.08 ± 0.03	6.12 ± 0.02	6.58 ± 0.02	6.28 ± 0.03	6.97 ± 0.02
k_ϕ^{\max} ($\times 10^{-3} \text{ h}^{-1}$)	4.3 ± 0.3	2.1 ± 0.2	12.0 ± 0.1	9.5 ± 0.4	6.4 ± 0.2	7.6 ± 0.1
k_2 ($\times 10^6 \text{ M}^{-1} \text{ h}^{-1}$)	5.4	0.13	6.7	1.8	2.5	0.60
$\log(k_2/k_2^0)$	0.18	-1.4	0.27	-0.29	-0.16	-0.78
$\log(k_2^{\max}/k_2^0)$	0.51	-0.41	0.27	-0.06	0.15	-0.33
$\log r = \log(k_2^{\max}/k_2^0)$	0.33	0.99	0.00	0.23	0.31	0.45

^aBecause of the experimental errors involved in pH, pK_a , k_ϕ^{\max} , and k_2^0 , the values for k_2 and the terms consisting of k_2 may involve an error of ~10%.

^bFor the calculations of $\log(k_2/k_2^0)$ and $\log(k_2^{\max}/k_2^0)$, we took $k_2^0 = 3.58 \times 10^6 \text{ M}^{-1} \text{ h}^{-1}$ measured for His5 of angiotensin III at a pK_a of 6.50.¹⁰

averaging the intensities of all the isotopic peaks across the area where all the relevant isotopic peaks are observed. In contrast, processing data with eq 4 has the difficulty of correcting the error caused by noise spikes superposed on either one of two specified isotopic peaks giving I_M and I_{M+1} , which are chosen to evaluate k_ϕ as a function of I_{M+1}/I_M , whereas each noise peak has the completely opposite effect on the value of I_{M+1}/I_M . The calculation involving the nonlinear term I_{M+1}/I_M is therefore avoidable particularly in MALDI MS where the need to process spectra consisting of peaks with relatively low S/N ratios often arises. Although the standard errors estimated for pK_a values were less than ± 0.03 (Table 1), a larger error could possibly arise if the standard deviation in k_ϕ and the change in pH readings during the H/D exchange reaction were taken into account. The more precise measurement would be achieved by increasing the frequency of sampling $\bar{I}_{M+i}(t)$ data at shorter time intervals to determine the slope k_ϕ .

The method presented here relies on the extremely high specificity of the H/D exchange reaction, which occurs uniquely at the $C^{\epsilon 1}$ -H group of the histidine residue among all the C-H groups in genetically encoded amino acid residues in D_2O under the conditions described here. Very few exceptions include the exchange of the C^α hydrogen of amino acid residue(s) during racemization. Under stringent conditions of incubation at pH 8 and 50 °C for 5 days in D_2O , incorporation of deuterium atoms into specific residues has been detected by LC-ESI-MS in a study of protein degradation due to racemization.¹⁹ This signifies that the H/D exchange

reaction at the $C^{\epsilon 1}$ position of a histidine residue is the sole chemical process not affecting the tertiary structure of proteins, as is the corresponding reaction at the amide N-H group. One of the advantages of the $C^{\epsilon 1}$ -H group over the amide N-H group in H/D exchange experiments is that it is stable not only to undesirable back-exchange but also to scrambling in MS/MS measurements.

Effects of 3'-CMP on k_ϕ^{\max} and pK_a of His Residues.

His12 and His119 located in the active site of RNase A are well-characterized as catalytic residues. According to the X-ray crystallography of RNase A and its complex with 3'-CMP [Protein Data Bank (PDB) entry 1RPF], the imidazole groups of His12 and His119 interact with the 3'-phosphate group of the competitive inhibitor at distances of 2.7 and 3.2 Å, respectively, through the formation of ion pairs (Figure 3A,B).²⁰ The titration curves in Figure 2 show the significantly large shift of the pK_a values to the alkaline region by as much as 1.4 pH units (5.7–7.1 for His12) and 0.7 pH unit (6.3–7.0 for His119) upon binding with the inhibitor (Table 1). This can reflect the change in the environment of these catalytic residues from the interaction with a basic group, probably the ϵ -amino group of Lys41, to that with the highly anionic phosphate group of 3'-CMP. The comparatively large pK_a shift due to the interaction with the phosphate group of the bound inhibitor has been observed for His12 and His119 in RNase A,³ His40 in RNase T₁,²¹ and His91 in RNase St (*Streptomyces erythreus*).¹³ In addition, a ¹H NMR study of wild-type and mutated (D121N and D121A) RNase A also revealed a similar effect of

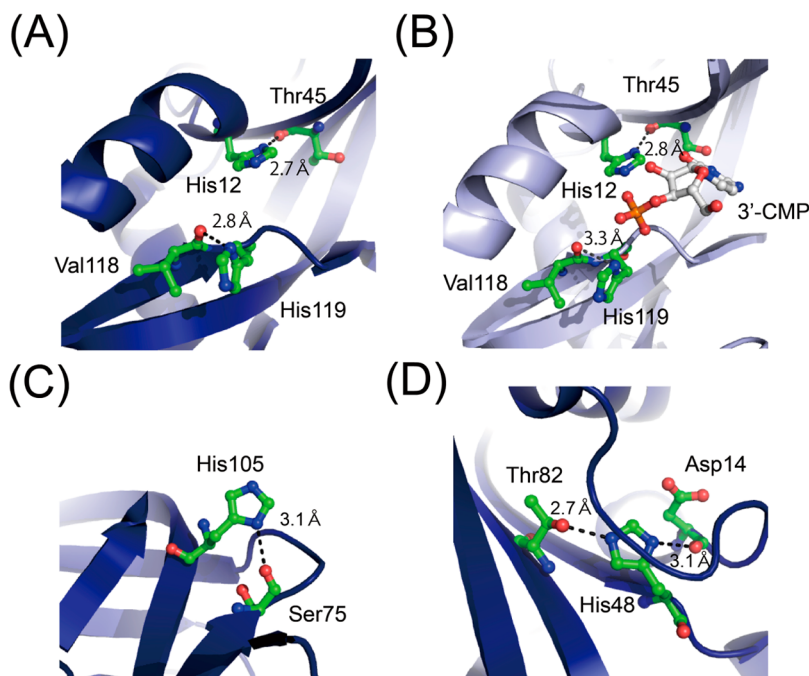


Figure 3. Environments of four histidine residues in the X-ray crystallographic structure of RNase A. (A) Imidazole groups of His12 and His119 are capable of forming hydrogen bonds with the main-chain carbonyl oxygen atoms of Thr45 and Val118, respectively, in the active site. (B) Both His12 and His119 can interact with the phosphate group of 3'-CMP, which binds to the enzyme in a manner that excludes some water molecules from the active site. (C) His105 is almost fully exposed to solvent on the surface of the molecule. Its imidazole group can form a hydrogen bond with the C-terminal Val124. (D) His48 is located just beneath the Ser19-Ala20-Ala21 chain in the loop loosely connecting two α -helices of residues 3–13 and 24–34. Its imidazole group is involved in a network of hydrogen bonds connecting Asp14 and Thr82. Figures are drawn using PDB entries 1RPH (A, C, and D) and 1RPF (B).²⁰ For space-filling models showing all four histidine residues, see Figure S3 of the Supporting Information.

uridine 3'-monophosphate on the pK_a shift of His12 and His119.²²

Together with the pK_a value, the k_{ϕ}^{\max} value probes the environment of a histidine residue as an index of the accessibility of the imidazole group to solvent molecules. As dictated by eq 7, however, the mutual dependency between pK_a and k_{ϕ}^{\max} values makes it difficult to compare the k_{ϕ}^{\max} values of two histidine residues with different pK_a values. For example, k_{ϕ}^{\max} values of His119 in the presence and absence of 3'-CMP were determined to be 0.0076 and 0.0064 h^{-1} (Table 1), respectively, as if the binding of 3'-CMP had enhanced the solvent accessibility of this residue. This is apparently inconsistent with the X-ray structure of the complex of 3'-CMP and RNase A, in which His119 must be shielded from bulk water by the bound inhibitor in the active site (Figure 3B).

The relationship between the k_{ϕ}^{\max} value and solvent accessibility would be represented more clearly if considered the second-order rate constant (k_2) as a parameter that is explicitly related to the H/D exchange reaction rate (ν) via the equation $\nu = k_2[\text{His}\cdot\text{D}^+][\text{OD}^-]$ (eq S-I-3 of the Supporting Information). From the experimental values of pK_a and k_{ϕ}^{\max} , we can obtain k_2 by transforming eq 7 to $k_2 = k_{\phi}^{\max} \times K_a/K_w$. The logarithmic form of this equation, in which the $\text{M}^{-1} \text{h}^{-1}$ dimension of k_2 has been removed by taking the ratio of k_2/k_2^0 for an appropriate imidazole derivative chosen to determine reference values of k_{ϕ} , $k_{\phi}^{\max(0)}$, and pK_a^0

$$\log(k_2/k_2^0) = \log[k_{\phi}^{\max}/k_{\phi}^{\max(0)}] - (pK_a - pK_a^0) \quad (6)$$

resembles the linear free energy relationship represented by a Brønsted equation

$$\log(k_2/k_2^0) = \alpha + \beta pK_a \quad (7)$$

that relates pK_a to the relative reactivity k_2/k_2^0 of a given functional group in model compounds, but not in proteins.²³ Indeed, the plot of $\log k_2$ versus pK_a measured for several small imidazole derivatives by the H/T exchange method yielded a straight line with a slope β of -0.7 .²⁴ With the slope of -0.7 determined empirically, the resulting Brønsted plot was successfully applied to the microenvironmental analysis of histidine residues in several proteins.^{12,13,21,24} Choosing His5 of angiotensin III as the reference representing the imidazole group fully accessible to bulk water with an H/D exchange rate constant k_2^0 of $3.58 \times 10^6 \text{ M}^{-1} \text{h}^{-1}$ [or $k_{\phi}^{\max(0)}$ of 0.0153 h^{-1}], which is maximal ($k_2 = k_2^{\max}$) at a pK_a of 6.50,¹⁰ we have a relationship

$$\log(k_2^{\max}/k_2^0) = 4.6 - 0.7pK_a \quad (8)$$

In the plot of $\log(k_2/k_2^0)$ versus pK_a , the line with a slope β of -0.7 (eq 7) runs through the point $\log(k_2/k_2^0) = 0$ at a pK_a of 6.50. As shown in Figure 4, all the data points for His12, -105, and -119 appear below or on the line represented by eq 8, suggesting that the deviation of k_2 from the maximal rate constant k_2^{\max} at the same pK_a value is a measure of structural interference imposed on the H/D exchange reaction. If we take the ratio $r = k_2^{\max}/k_2$, the extent of interference can be estimated on a logarithmic scale, $\log r$, as the vertical distance to be measured on the plot based on the equation derived from eq 8 in the following manner:

$$\begin{aligned} \log r &= \log(k_2^{\max}/k_2^0) - \log(k_2/k_2^0) \\ &= 4.6 - 0.7pK_a - \log(k_2/k_2^0) \end{aligned} \quad (9)$$

It is also possible to compare points $(k_{2(A)}, pK_{a(A)})$ and $(k_{2(B)}, pK_{a(B)})$ for two different histidine residues (or for a given

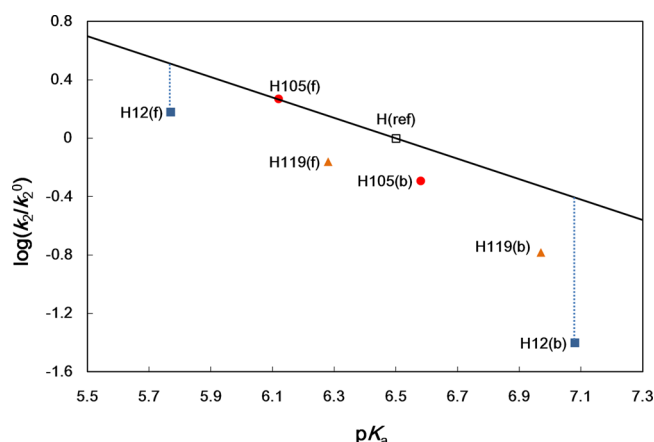


Figure 4. Brønsted plot for three histidine residues in RNase A in the H/D exchange reaction. Numerals following the letter H (histidine) refer to residue numbers and conditions: the enzyme in the absence (f, free) and presence (b, bound) of 3'-CMP. The line with the slope of -0.7 is drawn according to the equation $\log(k_2^{\max}/k_2^0) = 4.6 - 0.7\text{p}K_a$ (eq 8), so that the empty square [H(ref)] for His5 in angiotensin III falls at $\log(k_2/k_2^0) = 0$ and $\text{p}K_a = 6.50$. The vertical distance between a data point and the line with the slope of -0.7 represents $\log r$. Therefore, the difference in $\log r$ (the length of the blue dotted line) or $\Delta\log r_{(\text{free/bound})}$ for His12 corresponds to the difference in the lengths of the two dotted lines.

residue at different states), **A** and **B**, respectively, as the difference

$$\begin{aligned}\Delta\log r_{(\text{A/B})} &= \Delta\log r_{(\text{A})} - \log r_{(\text{B})} \\ &= 0.7[\text{p}K_{a(\text{B})} - \text{p}K_{a(\text{A})}] + \log[k_{2(\text{B})}/k_{2(\text{A})}]\end{aligned}\quad (10)$$

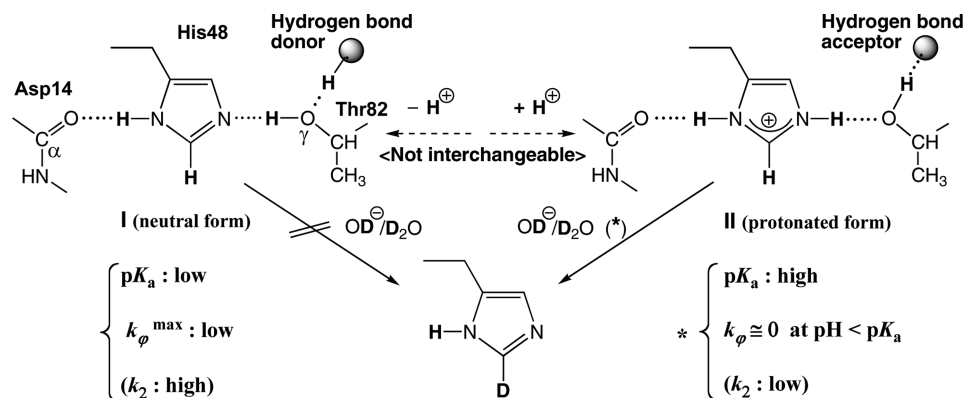
Note that the term $\Delta\log r_{(\text{A/B})}$ involves neither k_2^0 nor the corresponding $\text{p}K_a$, each of which may be determined for any histidine residue, yet it is convenient to choose k_2^0 for a histidine derivative in which the H/D exchange reaction is least likely to be interfered with, so that $\log r$ for each histidine residue can be estimated graphically on the Brønsted plot as shown in Figure 4. Although the similar linear relationship between $\log k_{\phi}^{\max}$ and

$\text{p}K_a$ for several imidazole derivatives has been suggested for the analysis of the solvent accessibility of histidine residues in a protein,²⁵ the use of the Brønsted plot drawn on the basis of eq 10 should allow the comparison of various histidine residues in different proteins.

Table 1 summarizes kinetic parameters $\log r$ along with the corresponding k_{ϕ}^{\max} and $\text{p}K_a$ values determined for three histidine residues (His12, -105, and -119) in RNase A in the presence and absence of 3'-CMP. As perceived from the Brønsted plot displaying $\log r = 0$ for His105 in the absence of 3'-CMP (Figure 4), the faster H/D exchange reaction rate of His105 compared to that of His5 in angiotensin III is reasonable if we allow for its relatively low $\text{p}K_a$ value of 6.1 and almost full exposure to solvent (Figure 3C).²⁰ Appreciable changes in $\log r$ and $\text{p}K_a$ for His105 may be related to a 180° flip of the imidazole ring upon binding of 3'-CMP with the enzyme, as one can recognize by a careful comparison of X-ray structures of PDB entries 1RPH and 1RPF (data not shown).²⁰ The apparent inconsistency between the enhanced pseudo-first-order rate constant (k_{ϕ}^{\max}) and possible solvent shielding effect on His119 upon binding with 3'-CMP could also be resolved by considering the increment of the $\log r$ value from 0.31 to 0.45, suggesting that the accessibility to solvent was suppressed 1.4-fold by inhibitor binding [$\Delta\log r_{(\text{free/bound})} = 0.45 - 0.31$ or $10^{0.45}/10^{0.31} = 1.4$]. Similarly, the increment in $\Delta\log r$ upon binding of 3'-CMP amounts to the 4.6-fold suppression of the H/D exchange rate [$\Delta\log r_{(\text{free/bound})} = 0.99 - 0.33$ or $10^{0.99}/10^{0.33} = 4.6$] for His12, which could be shielded from bulk water more effectively than His119 by the bound 3'-CMP. This is in good agreement with the X-ray crystal structure of RNase A in which His12 is at the bottom and His119 near the entrance of the active site cleft (see Figure 3A,B).²⁰

Considering that the H/D exchange reaction requires that the $\text{C}^{\epsilon 1}$ atoms be in direct contact with water, we may relate the value of k_{ϕ}^{\max} to the solvent accessibility of histidine residues.²⁵ However, the exchange rate of His48 was immeasurably slow throughout the pH range tested, despite its location just below the surface of the protein and thus it being incompletely shielded from solvent access (Figure S3 of the Supporting Information). As a possible factor responsible for the unexpectedly low H/D exchange rate of His48, we note the

Scheme 2. Possible Networks of Hydrogen Bonds Involving the Imidazole Group of His48 in Forms I (neutral) and II (protonated)^a



^aThe two forms of the imidazole group are distinguished by the orientations of the γ -OH bond of Thr82, making an ordinary acid–base equilibrium unlikely in a fixed conformational state. A possible hydrogen bond acceptor from the γ -OH group of Thr82 is the α -carbonyl oxygen of Gln101 (Figure S4 of the Supporting Information). Because $\text{C}^{\epsilon 1}$ H/D exchange occurs only when forms I and II are in an equilibrium characterized by constant K_a , the value of k_{ϕ} should be invariably zero regardless of the form (I or II) to which the imidazole group of His48 may be restricted.

two hydrogen bonds flanking the imidazole ring (Scheme 2). In this network of hydrogen bonds (Figure 3D), it is possible to assume that the imidazole group can take either the neutral (I) or the protonated (II) form, in which an acid–base equilibrium associated with the exchange of a proton between the imidazole ϵ_2 -nitrogen and the γ -oxygen atom of Thr82 is prohibited because of the nondissociable nature of the hydroxyl group. According to a ^1H NMR study of RNase A, the titration curves of the $\text{C}^{\delta 2}\text{-}^1\text{H}$ and $\text{C}^{\epsilon 1}\text{-}^1\text{H}$ resonances of His48 are discontinuous in the region from 5 to 7, indicating the possibility that there is a slow conformational transition with at least one intermediate form between the slowly exchanging base-stable and acid-stable conformers.^{3,26} In these base- and acid-stable conformers, His48 could possibly take forms I and II, respectively. It is therefore likely that the equilibrium between I and II forms occurs only in the suggested intermediate conformational form(s) but not in the base- and acid-stable conformers. As anticipated from the $\text{C}^{\epsilon 1}$ H/D exchange reaction mechanism, the value of k_{ϕ} should be invariably zero whichever form the imidazole group of His48 may take because there is no equilibrium between forms I and II, each of which belongs to a different conformational state. The similar rate-suppressing effect due to the restriction of the acid–base equilibrium could be expected to arise for the reaction of a metal-bound histidine residue.

As an additional factor to consider, a $\text{C}^{\epsilon 1}\text{H}\cdots\text{O}$ hydrogen bond can enhance or suppress the H/D exchange reaction. This effect was proposed to interpret the unusual ^1H NMR chemical shift of the $\text{C}^{\epsilon 1}$ proton resonance of a catalytic histidine residue in serine protease.²⁷ As far as four histidine residues in RNase A are concerned, however, no such unusual downfield shift has been reported in their ^1H NMR signals, despite the apparent short distance between the $\text{C}^{\epsilon 1}\text{H}$ and the possible hydrogen bond acceptor in His12 and His48 (data not shown). Nevertheless, this effect would be worth noting when there is a need to consider a rate-enhancing effect for the $\text{C}^{\epsilon 1}$ H/D exchange reaction at a specific site.

Native protein structure fluctuates thermally without needing a conformational transition. A large fluctuation allows water molecules to diffuse into the interior of a protein, thus enhancing the apparent solvent accessibility of a histidine residue that is completely shielded from the solvent otherwise. In particular, RNase A retains the catalytic activity without requiring that the intact native conformation be preserved. A few active forms of RNase A include various types of oligomers occurring in concentrated mildly acidic solutions^{27–30} and RNase S in a complex with the S-peptide.¹⁶ In the crystal of a domain-swapped dimer, the newly formed active site consists of His12 in the N-terminal segment of one chain and His119 in another chain.³¹ These examples suggest that allowance for conformational change at the active site is relatively large in this enzyme. This could explain, at least partly, the large variation of pK_a values reported for histidine residues in RNase A with different methods under a variety of solution conditions.^{3,26,32}

Although X-ray crystallographic structures provide us with information concerning solvent accessibility and noncovalent as well as covalent interactions, it is very difficult *a priori* to specify the major factor that modulates the histidine $\text{C}^{\epsilon 1}$ H/D exchange reaction, distinguishing among a variety of causes, including dynamic ones. To overcome such a difficulty, we need to implement the other methods for probing protein–ligand interaction and conformational stability such as conventional amide N H/D exchange, SUPREX,¹⁸ and fast photo-

chemical oxidation of a protein footprint (FPOP).³³ One of the common features of SUPREX and FPOP is that the measurements of kinetic parameters for individual histidine residues are conducted in the manner of bottom-up proteomics. The time scale covered by FPOP is on the order of microseconds, being much shorter than a range of days determined to be the typical half-life ($t_{1/2} = 0.693/k_{\phi}^{\text{max}}$) of the histidine H/D exchange reaction. By an appropriate combination of these complementary approaches, we could extend the method from the microenvironmental analysis of histidine residues in a folded protein to the exploration of protein interactions, protein folding and unfolding, and fluctuations occurring on the faster time scale. In line with this provision, we are refining parameters α and β in eq 7, so that we could interpret the values of $\log r$ and $\Delta\log r$ on a more quantitative basis.

CONCLUSION

We suggested a method based on MALDI MS to measure rate constant k_{ϕ} of the H/D exchange reaction occurring at the $\text{C}^{\epsilon 1}$ position of a histidine. The new data processing method was adapted to MALDI MS for the determination of k_{ϕ}^{max} and pK_a values for individual histidine residues in RNase A. To compare rate constants of histidine residues with different pK_a values, it was necessary to use second-order rate constant k_2 rather than k_{ϕ}^{max} because we could derive a pK_a -independent parameter, $\log(k_2^{\text{max}}/k_2)$, signifying the deviation of k_2 from k_2^{max} estimated from a linear free energy relationship (Brønsted plot) with the corresponding pK_a in the unperturbed state. For three of the four histidine residues, including His12 and His119, in the catalytic site, the possible effect of solvent accessibility on their $\log(k_2^{\text{max}}/k_2)$ values appeared to be consistent with the X-ray structures of RNase A in the presence and absence of 3'-CMP. In contrast, we found it impossible to interpret the extremely slow H/D exchange rate of His48 in terms of solvent accessibility alone because this residue is partially exposed to solvent just below the surface of the molecule. We conclude that the rate of the H/D exchange reaction at the imidazole ring C-2 (histidine $\text{C}^{\epsilon 1}$) position is affected not only by solvent accessibility but also by a network of hydrogen bonds involving both imidazole nitrogen atoms with nondissociable functional groups.

ASSOCIATED CONTENT

Supporting Information

Supplementary derivation of equations, mass spectra, and figures. This material is available free of charge via the Internet at <http://pubs.acs.org>.

AUTHOR INFORMATION

Corresponding Author

*Telephone and fax: +81-742-20-3396. E-mail: t.nakazawa@cc.nara-wu.ac.jp.

Funding

This study was supported in part by Grants-in-Aid for Scientific Research (Grant 21510225 to T.N. and Grant 22510230 to H.K.) from the Ministry of Education, Culture, Sports, Science and Technology of Japan.

Notes

The authors declare no competing financial interest.

REFERENCES

- (1) Englander, S. W., Mayne, L., Bai, Y., and Sosnick, T. R. (1997) Hydrogen exchange: The modern legacy of Linderström-Lang. *Protein Sci.* 6, 1101–1109.
- (2) Kaltashov, I. A., and Eyles, S. J. (2005) Mass spectrometry-based approaches to study biomolecular higher-order structure. In *Mass Spectrometry in Biophysics: Conformation and dynamics of biomolecules*, pp 143–323, John Wiley & Sons, Inc., Hoboken, NJ.
- (3) Markley, J. L. (1975) Correlation proton magnetic resonance studies at 250 MHz of bovine pancreatic ribonuclease. I. Reinvestigation of the histidine peak assignments. *Biochemistry* 14, 3546–3554.
- (4) Harris, T. M., and Randall, J. C. (1965) Deuterium exchange reactions at the C2-position of imidazoles. *Chem. Ind.* 41, 1728–1729.
- (5) Vaughan, J. D., Mughrabi, Z., and Wu, E. C. (1970) The kinetics of deuteration of imidazole. *J. Org. Chem.* 35, 1141–1145.
- (6) Amyes, T. L., Diver, S. T., Richard, J. P., Rivas, F. M., and Toth, K. (2004) Formation and stability of *N*-heterocyclic carbenes in water: The carbon acid pK_a of imidazolium cations in aqueous solution. *J. Am. Chem. Soc.* 126, 4366–4374.
- (7) Matsuo, H., Ohe, M., Sakiyama, F., and Narita, K. (1972) A new approach to the determination of pK_a's of histidine residues in proteins. *J. Biochem.* 72, 1057–1060.
- (8) Ohe, M., Matsuo, H., Sakiyama, F., and Narita, K. (1974) Determination of pK_a's of individual histidine residues in pancreatic ribonuclease by hydrogen-tritium exchange. *J. Biochem.* 75, 1197–1200.
- (9) Arata, Y., Shimizu, A., and Matsuo, H. (1978) A deuterium-labeling method for the assignment of histidine nuclear magnetic resonance peaks of proteins. *J. Am. Chem. Soc.* 100, 3230–3232.
- (10) Miyagi, M., and Nakazawa, T. (2008) Determination of pK_a values of individual histidine residues in proteins using mass spectrometry. *Anal. Chem.* 80, 6481–6487.
- (11) Kaplan, H. (1972) Determination of the ionization constants and reactivities of the amino-termini of α -chymotrypsin. *J. Mol. Biol.* 72, 153–162.
- (12) Kimura, S., Matsuo, H., and Narita, K. (1979) Hydrogen-tritium exchange titration of the histidine residues in bovine heart cytochrome *c* and analysis of their microenvironment. *Int. J. Pept. Protein Res.* 14, 472–478.
- (13) Miyamoto, K., Arata, Y., Matsuo, H., and Narita, K. (1981) Hydrogen-tritium exchange and nuclear magnetic resonance titrations of the histidine residues in ribonuclease St and analysis of their microenvironment. *J. Biochem.* 89, 49–59.
- (14) Lodowski, D. T., Palczewski, K., and Miyagi, M. (2010) Conformational changes in the G protein-coupled receptor rhodopsin revealed by histidine hydrogen-deuterium exchange. *Biochemistry* 49, 9425–9427.
- (15) Tran, D. T., Banerjee, S., Alayash, A. I., Crumbliss, A. L., and Fitzgerald, M. C. (2012) Slow histidine H/D exchange protocol for thermodynamic analysis of protein folding and stability using mass spectrometry. *Anal. Chem.* 84, 1653–1660.
- (16) Richards, F. M., and Vithayathil, P. J. (1959) The preparation of subtilisin-modified ribonuclease and the separation of the peptide and protein components. *J. Biol. Chem.* 234, 1459–1465.
- (17) Kuyama, H., Sonomura, K., and Nishimura, O. (2008) Sensitive detection of phosphopeptides by matrix-assisted laser desorption/ionization mass spectrometry: Use of alkylphosphonic acids as matrix additives. *Rapid Commun. Mass Spectrom.* 22, 1109–1116.
- (18) Ghaemmaghami, S., Fitzgerald, M. C., and Oas, T. G. (2000) A quantitative, high-throughput screen for protein stability. *Proc. Natl. Acad. Sci. U.S.A.* 97, 8296–8301.
- (19) Huang, L., Lu, X., Gough, P. C., and De Felippis, M. R. (2010) Identification of racemization sites using deuterium labeling and tandem mass spectrometry. *Anal. Chem.* 82, 6363–6369.
- (20) Zegers, I., Maes, D., Dao-Thi, M.-H., Poortmans, F., Palmer, R., and Wyns, L. (1994) The structures of RNase A complexed with 3'-CMP and d(CpA): Active site conformation and conserved water molecules. *Protein Sci.* 3, 2322–2339.
- (21) Arata, Y., Kimura, S., Matsuo, H., and Narita, K. (1979) Proton and phosphorus nuclear magnetic resonance studies of ribonuclease T₁. *Biochemistry* 18, 18–24.
- (22) Quirk, D. J., and Raines, R. T. (1999) His...Asp catalytic dyad of ribonuclease A: Histidine pK_a values in the wild-type, D121N, and D121A enzymes. *Biophys. J.* 76, 1571–1579.
- (23) Creighton, T. E. (1993) in *Proteins: Structure and molecular properties*, 2nd ed., pp 274–275, Freeman and Co., New York.
- (24) Minamino, N., Matsuo, H., and Narita, K. (1978) Tritium exchange titration of imidazole derivatives: Factors affecting on pK_a and reactivity of imidazole ring. In *Peptide Chemistry 1977* (Shiba, T., Ed.) pp 85–90, Protein Research Foundation, Osaka, Japan.
- (25) Mullangi, V., Zhou, X., Ball, D. W., Anderson, D. J., and Miyagi, M. (2012) Quantitative measurement of the solvent accessibility of histidine imidazole groups in proteins. *Biochemistry* 51, 7202–7208.
- (26) Markley, J. L. (1975) Correlation proton magnetic resonance studies at 250 MHz of bovine pancreatic ribonuclease. II. pH and inhibitor-induced conformational transitions affecting histidine-48 and one tyrosine residue of ribonuclease A. *Biochemistry* 14, 3554–3561.
- (27) Ash, E. L., Sudmeier, J. L., Day, R. M., Vincent, M., Torchilin, E. V., Haddad, K. C., Bradshaw, E. M., Sanford, D. G., and Bachovchin, W. W. (2000) Unusual ¹H NMR chemical shifts support (His) C^ε1-H...O=C H-bond: Proposal for reaction-driven ring flip mechanism in serine protease catalysis. *Proc. Natl. Acad. Sci. U.S.A.* 97, 10371–10376.
- (28) Crestfield, A. M., Stein, W. H., and Moore, S. (1962) On the aggregation of bovine pancreatic ribonuclease. *Arch. Biochem. Biophys., Suppl.* 1, 217–222.
- (29) Libonati, M., and Gotte, G. (2004) Oligomerization of bovine ribonuclease A: Structural and functional features of its multimers. *Biochem. J.* 380, 311–327.
- (30) Liu, Y., Hart, P. J., Schlunegger, M. P., and Eisenberg, D. (1998) The crystal structure of a 3D domain-swapped dimer of RNase A at a 2.1-Å resolution. *Proc. Natl. Acad. Sci. U.S.A.* 95, 3437–3442.
- (31) Liu, Y., Gotte, G., Libonati, M., and Eisenberg, D. (2001) A domain-swapped ribonuclease A dimer with implication for amyloid formation. *Nat. Struct. Biol.* 8, 211–214.
- (32) Antosiewicz, J., McCammon, J. A., and Gilson, M. K. (1996) The determinants of pK_s in proteins. *Biochemistry* 35, 7819–7833.
- (33) Gau, B. C., Sharp, J. S., Rempel, D. L., and Gross, M. L. (2009) Fast photochemical oxidation of protein footprints faster than protein unfolding. *Anal. Chem.* 81, 6563–6571.

NOTE ADDED AFTER ASAP PUBLICATION

This paper was published ASAP on March 14, 2014. Eq 10 has been updated, and the corrected version was reposted on March 25, 2014.